The Study of Bio-Inspired Robot Motion Control System

Takayuki Matsuo, Takeshi Yokoyama, Daishi Ueno, Kazuo Ishii

Abstract:

Robots and robotics technologies are expected as new tools for inspection and manipulation. The dynamics of robot always are changed by environment and robot of state in mission. Therefore, an adaptation system, which is able to switch controller due to environment and robot of state, is needed. Meanwhile, animals are able to go through several environments and adapt several own states. The adaptation system is realized Central Pattern Generator (CPG). CPG exists in nervous system of animals and generates rhythmical motion pattern. In this paper, a robot motion control system using CPG is proposed and applied to an amphibious multi-link mobile robot.

Keywords: *CPG, snake-like robot, biomimetics.*

1. Introduction

Robot and robotics technologies are expected to provide new tools for inspection and manipulation. The dynamics of Robot is changed by environment and state of robots: weight, attitude and so on. Operations in several environments and conditions of robot need switching system, which is able to change due to a variety of circumstances. The system, which is worked, is called "Hybrid Dynamical System (HDS)". HDS is able to manage many-controlled object. Therefore, one is very complex theory. But, in the nature, Animals are able to move and adapt between different environments. Adaptation system of animal is realized by Central Pattern Generator (CPG). CPG exists in nervous system of animal and generates rhythmical pattern. Several motion patterns of animals such as swimming, waking, flapping and so on are generated by CPG. CPG has "entrainment feature" which synchronizes a wave that matches the resonance frequency. The wave of CPG is able to be adjusted using sensory feedback. Taga [1] realized simulation of biped walking robot based on the idea that motion pattern is generated by interaction between CPG, body-dynamics and environment. Williamson [2] applied CPG to a humanoid robot that performs cranking, sawing, and hitting drum. Matsuoka *et al.* [3] developed control system of a giant swing robot which is switched among swing mode and rotation mode using CPG. The goal of our study is development of bio-inspired robot control system using CPG and application into HDS. In this paper, we report about development of an amphibious multi-link mobile robot for test bed of HDS and dynamics property analysis. Additionally, distributed motion control system using entrainment feature of CPG without sensory feedback was developed.

2. Development of Amphibious Multi-Link Mobile Robot "AMMR"

2.1. Motion of snake-like animals

In previous works, Hirose *et al.* developed multi-link mobile robot [4] and underwater multi-link mobile robot [5]. These robots move forward using reaction forces from frictional force on ground or fluid drag force in underwater. Robot dynamics are different between ground motion and underwater motion. Especially, an amphibious multi-link mobile robot[6] is very interesting for HDS to apply CPG. In this research, we applied motion control system using CPG to amphibious multi-link mobile robot. The motion mechanisms of snake-like animals have already been studied by Hirose [7] and Azuma [8]. A snake's body is covered with special scales that have low friction in the tangential direction and high friction in the normal direction. This feature enables thrust to be produced from a wriggle motion. An eel swims under water by generating an impellent force from a hydrodynamic force. Snake and eel generate impellent force actuating each joint with a certain phase difference. And, at turning motion, joint trajectories of snake and eel have bias, which is balance of oscillation of joint.

2.2. Mechanism

In our previous work [9], we developed the multi-link mobile robot, as a test bed for the evaluation of a motion control system using a CPG. We realized wriggle motion for forward and turning motions using periodical output signals of the CPG control system. However, the multi-link mobile robot was not able to evaluate HDS in which the dynamics of a robot transfer from one mode to another because previous one was not able to move in underwater. In previous works, electrical circuit did not have feedback connection because servomotors, which were not able to extract angle data, were used. Thus we developed an amphibious multi-link mobile robot (see Fig. 1) as a new test bed for motion control and adaptation in two different environments that require different dynamics: land and underwater environments. Table 1 gives the specifications of an amphibious multi-link mobile robot. An amphibious multi-link mobile robot moves both over land and under water. Therefore, waterproofness is an important design consideration. O-rings are employed on the shaft of each joint and under the cylinder lids to ensure the waterproofness of the robot. The robot comprises eight cylinders that are joined so that each cylinder can rotate around a yaw axis via DC motors, a gearbox and a control circuit, as shown in Fig. 2. A range of joint movement is $\pm\pi/3$[rad]. Hydrodynamic forces produced

by fins and the body produce thrust forces under water and passive wheels are used on ground (Fig. 3).

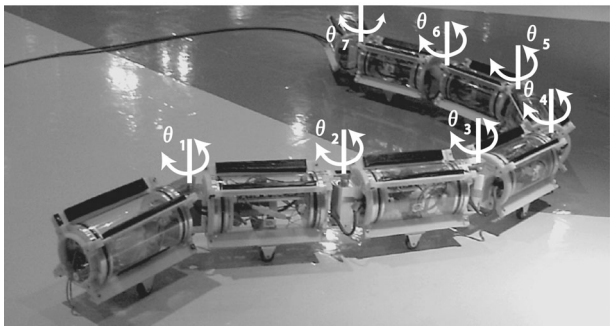

Fig. 1. Overview of AMMR.

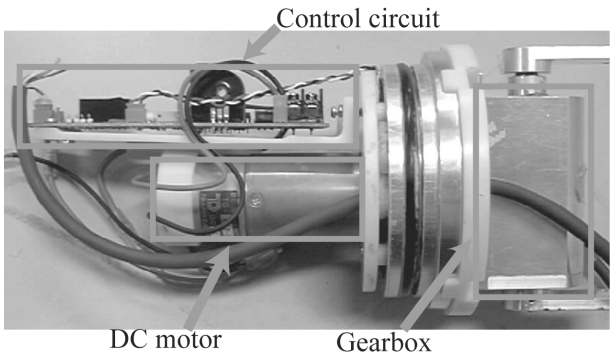

Fig. 2. Internal architecture of a motor module.

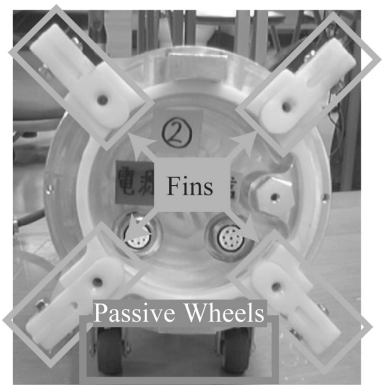

Fig. 3. Passive Wheels and Fins.

2.3. Electrical system

An amphibious multi-link mobile robot consists of two kinds of cylinders: a cylinder for the head (head module) and seven cylinders for the body (motor modules). Main voltage for each module is 8 V and decrease voltage into 5 V for MPU and sensors using DC/DC converter. However, connection method of power line is a cascade connection. Therefore, voltage decreases from tail to head module. One cannot evaluate torque of each joint in this condition. As main power, 24 V are used and voltage is stepped down to 8 V in each module using switching regulator, which is able to apply high electrical current. A motor module has a motor to control the joint angle and a circuit board. The circuit has a microprocessor unit (MPU, PIC18F452), a potentiometer to measure the joint angle, an RS485 transceiver (MAX1487) for communication and a current sensor to measure joint torque. The MPU calculates the target trajectory using the neuron potential of the CPG or sinusoidal function, controls the motor using a PID control, manages sensor information (e.g., current and angle data) and communicates with circuits of other modules using the RS485. The head module transfers the target behavior to other modules and control of communication.

3. The experimental analysis of dynamics property for "AMMR"

3.1. Method of dynamics property analysis

In this paper, dynamics property analyses are carried out in 120 motion patterns which are expressed by combination of amplitude a (between 10 deg and 60 deg with a step of 10 deg), frequency f (between 0.1 Hz and 0.4 Hz with a step of 0.1Hz) and phase difference φ (between 20 deg and 100 deg with a step of 20 deg) on ground and in underwater. For dynamics property analyses, travel velocity v m/s and dissipation power per a meter ΔW J/m of robot analyses were evaluated by average value of 3 trials in each motion pattern. And a motion capture system was used for measurements of robot motion. 8 markers are put on head, tail and joints of robot and these markers were tracked by a motion capture system. Travel distance of head and tail markers in a straight line d^h, d^t m were measured and average of d^h and d^t was defined as travel distance d m of robot. Travel velocity v m/s is evaluated from travel distance d and operation time t=20 s.

Table 1. Specification of robot.

Length [m]	2.2	Communication	RS485
Weight [kg]	15.6	Sensors	Current sensor (LTS 6-NP) Potentiometer
Number of joints	7		
Operation depth [m]	10	Actuator	DC motor (05D-SU TUKASA)
MPU	PIC18F452	Motor driver	TA8440H

Dissipation powers per travel distance of a meter ΔW J/m were evaluated from total dissipation power W J in operation time t=20 s and travel distance d m as shown in Eq. (2) and total dissipation power were defined as Eq. (1). V V and $I(n)$ A shows impressed voltage and carried electrical current of motor per sampling time Δt=0.05 s.

$$W = \sum_{i=1}^{7} \sum_{n=1}^{step} VI(n)\Delta t \tag{1}$$

$$\Delta W = \frac{W}{d} \tag{2}$$

3.2. Velocity analysis on ground and underwater

Fig. 4a)-d) and Fig. 5a)-(d) show velocities of robot on ground and in underwater by adjustment of a deg and φ deg at four fixed frequencies of f=0.1, 0.2, 0.3 Hz and 0.4 Hz. Velocities were expressed by brightness and the brighter grids are the faster velocity. In ground motions, velocities were fast in white grids and fastest velocity was v=0.54 m/s at f=0.4 Hz, a=30 deg, φ=40 deg]. Travel velocities v m/s were fast at t a=30, 40 deg by adjusting a deg and by adjusting phase difference φ deg, travel velocities v m/s were fast at φ=40 deg.

Meanwhile, in underwater motion, fastest velocity was v=0.10m/s in white grids. Travel velocities v m/s are fast at a=50 deg by adjusting a deg and by adjusting phase difference φ deg, travel velocities v m/s were fast at φ=60 deg. The parameters, which generate maximum velocity, were difference between ground motion and underwater motion. Robot was not able to move in parameter which include a=10 deg and φ=20 deg.

Next, we focused on variations of velocities. Fig. 6a)-c) shows examples of variations of velocities in ground motions. Fig. 6a) shows variations of velocities by adjustment of φ deg and a deg at fixed parameter of f=0.4 Hz, Fig. 6b) shows variations of velocities by adjustment of f Hz and a deg at fixed parameter of φ=40 deg and Fig. 6c) show variations of velocities by adjustment of a deg and f Hz at fixed parameter of φ=40 deg. Fig. 7a)-c) shows examples of variations of velocities in underwater motion at same parameters as ground motions. On ground, velocities are changed by adjustment φ and f, however velocities were not changed or changed a few by adjusting a between a=40 deg and a=60 deg. Velocities became max speed at φ=40 deg and f=0.4 Hz. These results show that adjustment of φ and f are more effective than adjustment of a in control of velocity on ground. Robot snakes its way, therefore, definition of velocity is different whether to define the distance in straight line which robot moves

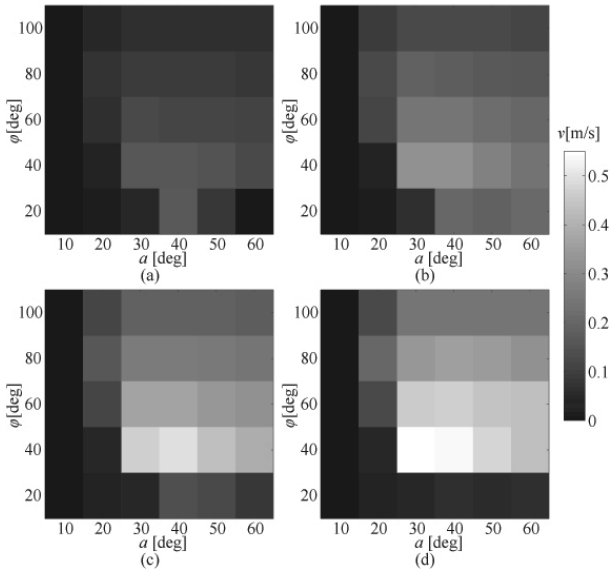

Fig. 4. Variations of travel velocity in ground motions (a) f=0.1[Hz] (b)f=0.2[Hz] (c)f=0.3[Hz] (d)f=0.4[Hz].

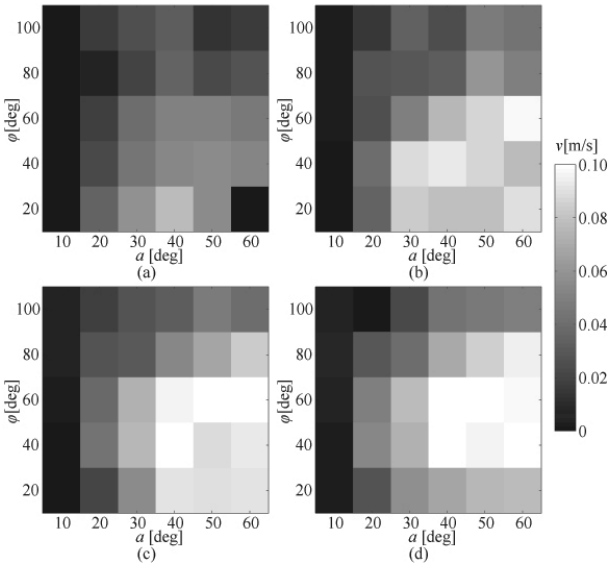

Fig. 5. Variations of travel velocity in underwater motions (a) f=0.1[Hz] (b)f=0.2[Hz] (c)f=0.3[Hz] (d)f=0.4[Hz].

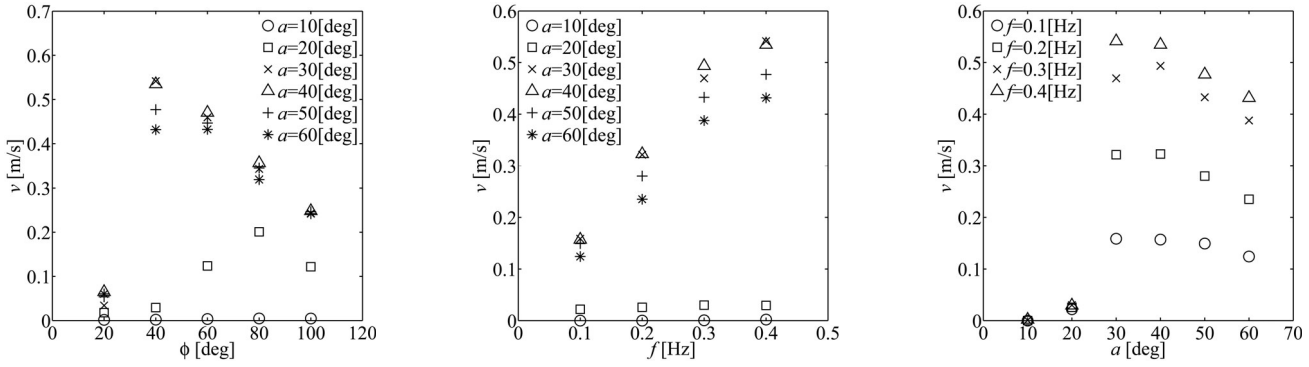

Fig. 6. Variations of travel velocity on Ground.

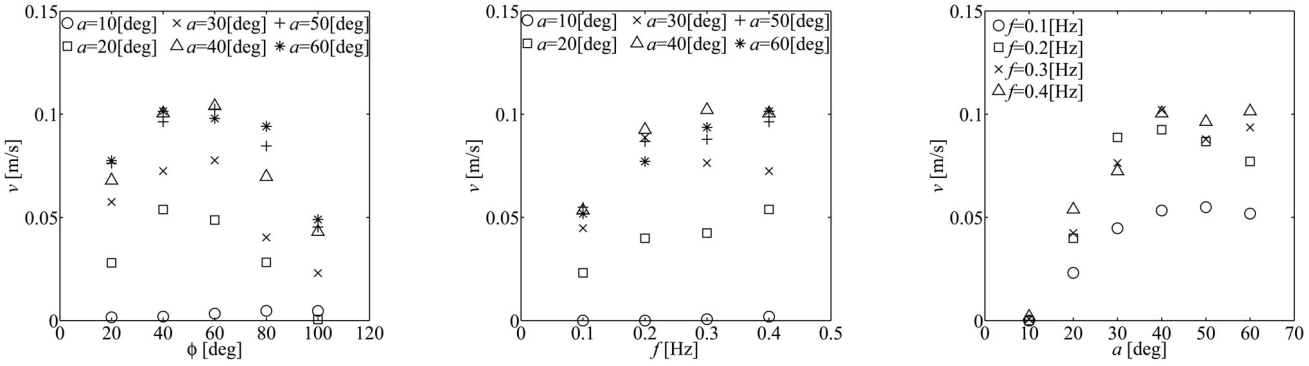

Fig. 7. Variations of travel velocity in Underwater.

as travel distance or define the distance which robot snakes its way as one. In this paper, the distance in straight line which robot moves is defined as travel distance. Therefore, velocities were not changed so much by adjustment of a. In underwater, velocities are changed by adjustment φ, f and a. Velocity became max speed at φ=60 deg and f=0.3 Hz. In underwater, robot is affected from fluid drag force. Fluid drag force becomes big value if velocity and acceleration of robot are big value. Therefore, robot velocity decreased in high frequency (f=0.4 Hz).

3.3 Dissipation power analysis on ground and underwater

Fig. 8a)-d) and Fig. 9a)-d) shows results that dissipation power per travel distance of a meter ΔW J/m was analyzed. In the analysis, ΔW is shown by brightness like velocity analysis. The brighter grid is the lower value. In the result of analysis, on ground, the lowest value was 23.49 J/m at a=30 deg, f=0.4 deg, φ=80 deg. Meanwhile, in underwater, the lowest value was 103.74 J/m at a=60 deg, f=0.2 deg, φ=60 deg. Fig. 10a)-c) and Fig. 11a)-c) show examples of variation of dissipation power per travel distance of a meter. Fig. 10a)-c) and Fig. 11a)-c) don't include data at a=10 deg because robot was not able to go forward so much. Overall, underwater motions need more power than ground motions. As shown in Fig. 10a) and Fig. 11a), if phase difference φ is adjusted from 20 to 100 deg, ΔW becomes minimum value at ϕ=60 deg on ground and ϕ =80 deg in underwater. As shown in Fig. 10b) and Fig. 11b), if frequency f is adjusted from 0.1 to 0.4 Hz, ΔW becomes minimum value at f=0.3 Hz on ground and f=0.4 Hz in underwater.

4. Motion control system using CPG

4.1. CPG Models

Several CPG models are proposed such as Von der Pol [10] model, Matsuoka model [11],[12], Terman-Wang model [13], Willson-Cowan model [14], and so on. We employed Matsuoka model. The Matsuoka model is expressed in Eqs. (3)–(5), where u_i is the membrane potential of the *i-th* neuron, v_i represents the degree of adaptation, u_0 is the external input with a constant rate, f_i is the feedback signal from a sensory input, τ_u, τ_v and β are parameters that specify the time constant for the adaptation, w_{ij} is the neuron weighting, y_i is output of neuron and n is the number of neurons. The CPG wave in the Matsuoka model can entrain external oscillatory input using sensor input f_i. The neural oscillator wave is able to entrain a wave that matches the resonance frequency. Additionally, the wave in the Matsuoka model is able to change amplitude and bias by adjusting u_0.

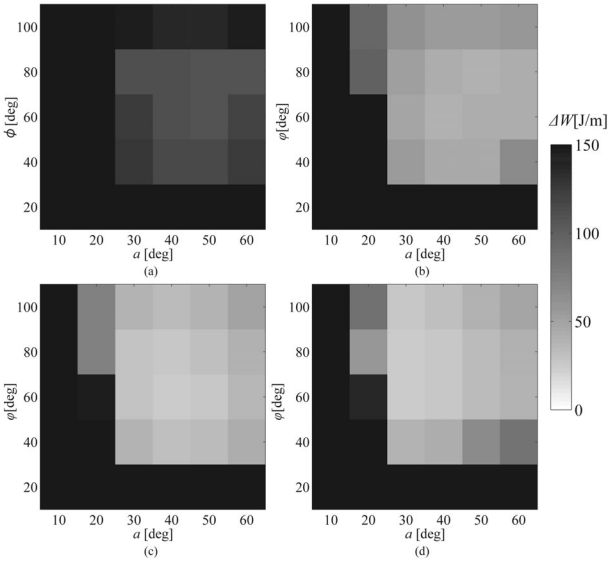

Fig. 8. Variations of dissipation power in ground motions (a)f=0.1[Hz] (b)f=0.2[Hz] (c)f=0.3[Hz] (d)f=0.4[Hz].

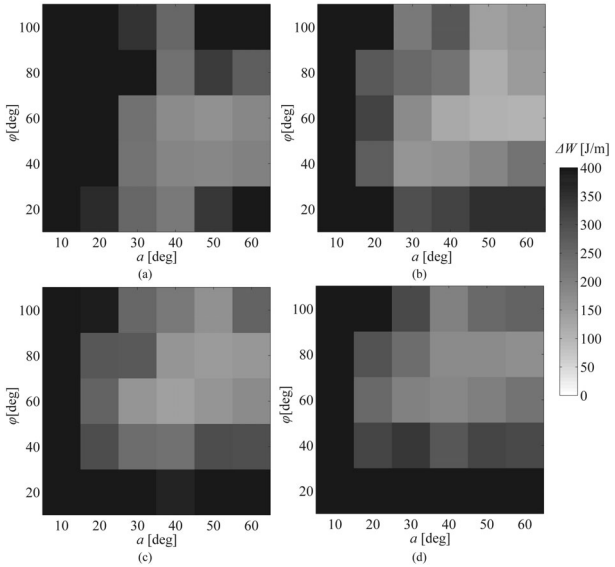

Fig. 9. Variations of dissipation power in underwater motions (a) f=0.1[Hz] (b)f=0.2[Hz] (c)f=0.3[Hz] (d)f=0.4[Hz].

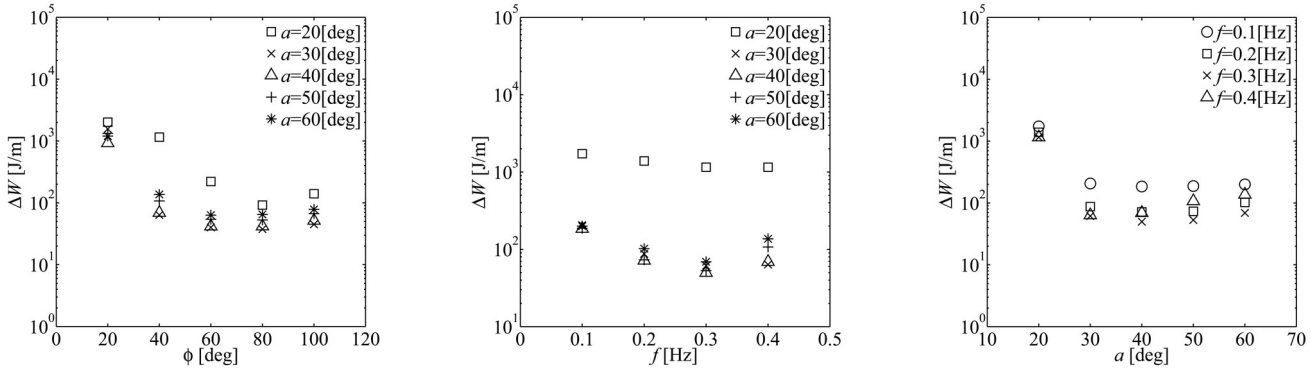

Fig. 10. Variation of Dissipation Power on Ground.

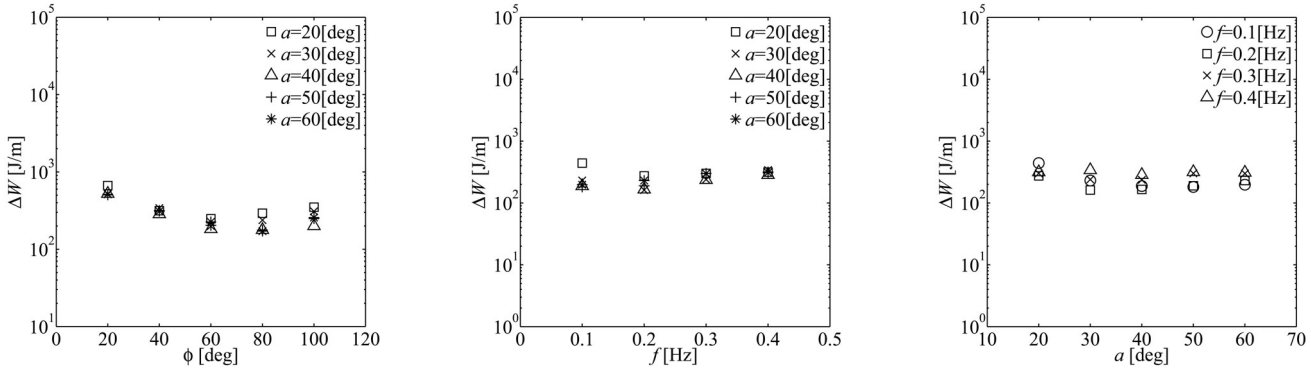

Fig. 11. Variation of Dissipation Power in underwater.

In this paper, we realized wave generation, which has phase difference and shift neutral position of wave oscillation adjusting CPG parameters such as τ_u, τ_v and u_0 are used for motion control.

$$\tau_v \dot{v}_i = -v_i + y_i \tag{3}$$

$$\tau_u \dot{u}_i = u_i - \beta v_i + \sum_{j=1}^{n} w_{ij} y_i + u_0 + f_i \tag{4}$$

$$y_i = \max(0, u_i) \tag{5}$$

4.2. Design of Motion Control System Using CPG

The CPG for the multi-link mobile robot is shown in Fig. 12. A neural oscillator consists of an extensor neuron (EN_k) and a flexor neuron (FN_k), which connects each other through the weights of w_{ef} and w_{fe}. k means neural oscillator number. Extensor neurons are connected to flexor neurons of the neighboring neural oscillator, and flexor neurons are connected to extensor neurons of the neighboring neural oscillator. We defined weights between neural oscillators as w_1 and w_2. And, an external input of extensor neuron and flexor neuron are defined as u_{0_e} and u_{0_f}. A set of neural oscillator is assigned to each of our robot's seven joints. Taga[15],[16] simulated biped walking robot connecting neural oscillator to musculoskeletal model. In this paper, we used same method as neural oscillator model. The output of neural oscillator O_k follows Eq. (6). The network architecture is designed as a closed loop to generate periodically successive signals with a certain phase. After CPG simulations, we employed sets of CPG parameters for generating waves with a certain phase difference and CPG waves are converted into target joint angles following Eq. (7). Table 2 gives the parameters for forward motion and Fig. 13 shows target joint angles, which are made by CPG wave. The amplitude a of target joint angles are 40 deg and frequency f is 0.1 Hz. We determined the parameters through trial and error using Matlab. We simulated and calculated equation of Matsuoka model adjusting parameters for finding parameter sets, which are able to generate waves. And we determined parameter sets which are able to realize a certain amplitude, phase difference and frequency. Amplitude and frequency of target joint angles are linked to robot's speed. If amplitude and frequency are set large value, robot's speed becomes fast. On the contrary, if their values are set to be small, robot's speed becomes slow. The motion control system changes frequency adjusting τ_u and τ_v and changes amplitude adjusting u_{0_e} and u_{0_f}. Table 3 shows the relationship between τ_u, τ_v and frequency. Other parameters are same with Table 2. Table 4 shows the relationship between u_{0_e}, u_{0_f} and amplitude. Other parameters are same with Table 2. The amphibious multi-link mobile robot can change direction with a change in parameter u_{0_e} and u_{0_f}, which shifts the neutral position. If parameters are set u_{0_e} =0.99 and u_{0_f} =0.94, the robot turns and moves toward the right. Figure 14 shows the output of the CPG network, which has bias 15 deg for a right turn motion. If u_{0_e} and u_{0_f} are adjusted, bias is changed. Table 5 shows the variations in bias.

$$O_k = y_{ek} - y_{fk} \tag{6}$$

$$\hat{\theta}_k = 100 * O_k \tag{7}$$

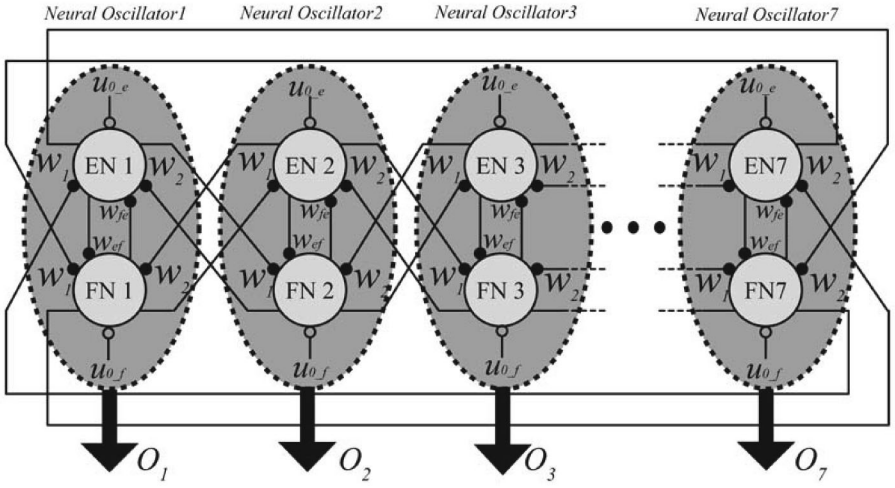

Fig. 12. A CPG architecture of robot.

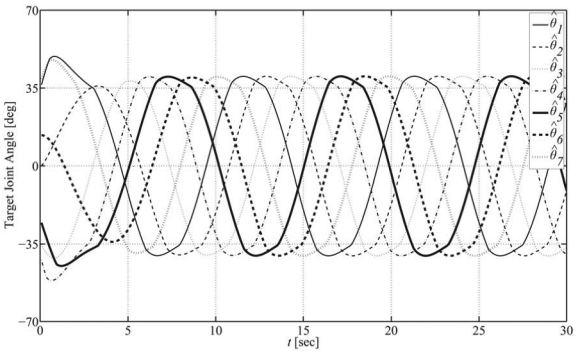

Fig. 13. Output of CPG for forward motion.

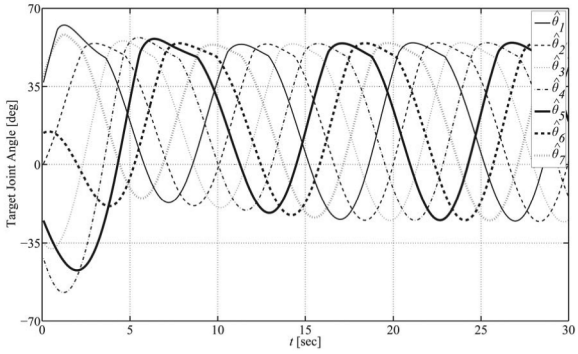

Fig. 14. Output of CPG for right turn.

Table 2. Parameters of CPG in forward motion.

τ_u	1.08	τ_v	1.18	β	1
w_{ef}	1.5	w_{fe}	1.5	W_1	0.3
W_2	0	u_{0_e}	0.71	u_{0_f}	0.71

Table 3. Parameters for adjustment of frequency.

f [Hz]	τ_u	τ_v
0.1	1.08	1.18
0.2	0.54	0.59
0.3	0.36	0.41
0.4	0.27	0.29

Table 4. Parameters for adjustment of amplitude.

a [deg]	u_{0_e} and u_{0_f}	a [deg]	u_{0_e} and u_{0_f}
10	0.17	40	0.71
20	0.35	50	0.88
30	0.53	60	1.06

Table 5. Parameters for adjustment of bias.

Bias [deg]	u_{0_e}	u_{0_f}
5	0.79	0.76
10	0.89	0.85
15	0.99	0.94

5. Conclusions

In this paper, an amphibious multi-link mobile robot that has seven joints and moves on ground and under water was developed. And dynamics property analysis was carried out on ground and in underwater. Velocity was max speed at a=30 deg f=0.4 Hz ϕ=40 deg on ground and at a=40 deg f=0.3 Hz ϕ=60 deg in underwater. Additionally, a distributed robot motion control system using a CPG was developed and realized forward and turning motion. In future work, we will include a sensor feedback in the bio-inspired robot motion control system.

ACKNOWLEDGMENTS

This work was supported by a 21st Century Center of Excellence Program, "World of Brain Computing Interwoven out of Animals and Robots (Pl: T. Yamakawa)" (center#J19) granted to the Kyushu Institute of Technology by the Ministry of Education, Culture, Sports, Science and Technology of Japan.

AUTHORS

Takayuki Matsuo*, Daishi Ueno, Kazuo Ishii - Department of Brain Science and Engineering, Kyushu Institute of Technology, 2-4 Hibikino, Wakamatsu, Kitakyushu, Fukuoka, 808-0196, Japan. Tel&Fax: +81-93-695-6102. E-mail: t-matsuo@brain.kyutech.ac.jp.

Takeshi Yokoyama - YASUKAWA Electric Co. 2-1, Kurosaki-shiroishi, Kitakyushu, Fukuoka, 806-0004, Japan.

* Corresponding author

References

[1] Taga G., "Emergence of Locomotion", *J. of R.S.J.*, vol. 15, no. 5, 1997, pp. 680-683 (in Japanese).

[2] Williamson M.M., *Robot Arm Control Exploiting Natural Dynamics*, PhD thesis, Massachusetts Institute of Technology, 1999

[3] Matsuoka K., Ohyama N., Watanabe A., Ooshima M., "Control of a giant swing robot using a neural oscillator", *Advances in Natural Computation* (Proc. ICNC 2005, Part II), 2005, pp.274-282.

[4] Mori M., Yamada H., Hirose S., "Design and Development of Active Cord Mechanism "ACM-R3" and its 3-dimentional Locomotion Control", *J. of R.S.J.*, vol. 23, no. 7, 2005 , pp. 886-897 (in Japanese).

[5] Takayama T., Hirose S., "Study on 3D Active Cord Mechanism with Helical Rotational Motion", *J. of R.S.J.*, vol. 22, no.5, 2004, pp.625-635 (in Japanese).

[6] Chigasaki S., Mori M., Yamada H., Hirose S., "Design and Control of Amphibious Snake-Like Robot "ACM-R5"". In: *Proceedings of the 2005 JSME Conference on Robotics and Mechatronics*, ALL-N-020(1)-(3).

[7] Hirose S., "*Bionic machine engineering*", Kougyo Chosakai, 1987 (in Japanese).

[8] Azuma A., *The subject-book of Animal's Motion*, Asakura, 1997.

[9] Matsuo T., Yokoyama T., Ishii K., "Development of Neural Oscillator Based Motion Control System and Applied to Snake-like Robot". In: *IROS'07*, 2007, pp. 3697-3702.

[10] Val der Pol B., "On relaxation oscillations", *Phil. Mag.*, vol. 2, no.11, 1926, pp. 978-992.

[11] Matsuoka K., "Sustained oscillations generated by mutually inhibiting neurons with adaptation", *Biological Cybernetics*, vol. 52, 1985, pp. 367-376.

[12] Matsuoka K., "Mechanisms of frequency and pattern control in the neural rhythm generators", *Biological Cybernetics*, vol. 56, 1987, pp. 345-353.

[13] Terman D., Wang D.L. ,"Global competition and local cooperation in a network of neural oscillators", *Physica D81*, 1995, pp. 148-176.

[14] Wilson H.R., Cowan J.D., "Excitatory and inhibitory interactions in localized populations of model neurons", *Biological Journal*, vol. 12, 1972, pp. 1-24.

[15] Taga G., Yamaguchi Y., Shimizu H., "Self-organized control of bipedal locomotion by neural oscillators in unpredictable environment", *Biological Cybernetics*, vol. 65, 1991, pp. 147-159.

[16] Taga G., "A model of the neuro-musculo-skeletal system for human locomotion II. Real-time adaptability under various constraints", *Biological Cybernetics*, vol. 73, 1995, pp. 113-121.